



# Behavior of self-compacting recycled aggregate concrete filled double skin steel tubular square columns under axial loading

Zain AL-abdeen Injers Tomma<sup>a</sup> and Samoel Mahdi Saleh<sup>a</sup>

<sup>a</sup>College of Engineering, University of Basrah, Basrah 61004, Iraq

\*Corresponding author E-mail: [zainalmaliky451@gmail.com](mailto:zainalmaliky451@gmail.com)

DOI:10.52113/3/eng/mjet/2025-13-01-/51-65

## Abstract

A series of experimental tests were carried out to investigate the behavior of sustainable self-compacting concrete-filled double skin steel tubular (HSCFDST) columns. Nine column specimens were tested in the present study, taking into account the effects of the inner shape of the column cross section (circular or square), the hollowness ratio, and the recycled aggregate replacement ratio. For comparison, three of the tested specimens were filled with normal recycled aggregate concrete. It was observed that the maximum axial strength of CFDST columns increases with the increase in void fraction for round inner tubes and decreases with the increase in void fraction for square inner tubes. Also, it was found that for square column specimens, the ultimate axial strength of HSCFDST columns was inversely proportional to their hollowness and slenderness ratios. CFDST column specimens filled with recycled aggregate concrete compared with those filled with normal aggregate concrete decreased stiffness and ultimate axial strength but gave unexpected results for the ultimate axial strength; therefore, the suitable choice for the section properties of the inner steel tube is required. The bearing capacity of CFDST square columns with concrete aggregate (30% and 60%) decreases by 5% and 10%, respectively. Increasing the volume of recycled concrete led to a decrease in maximum load capacity, with a 30% volume resulting in a 5%-10% reduction and 60% volume further reducing capacity by 10%-14.6%. The experimental results and analytical approach that were developed by other researchers showed good agreement.

**Keywords:** CFDST, Sustainable concrete, self-compacting concrete, Composite column, Hollowness ratio, recycled aggregate

## 1. Introduction

High-rise structures are becoming commonplace due to the growing population and industrial need for residential and commercial space. The use of reinforced concrete in high-rise buildings has resulted in the construction of larger structural elements, which has reduced the structure's aesthetic appeal. As a result, there is a search for more suitable materials and profiles, such as so-called composite structures. The advantages of both steel and concrete are combined in steel-concrete composite buildings, which combine the inherent mass, stiffness, damping, and cost-effectiveness of concrete with the strength, and lightweight nature of steel. A new type of composite construction is steel-concrete composite columns. They are commonly used due to their significant energy absorption capacity, effective material utilisation, enhanced stiffness and ductility, and huge weight-bearing capacity [1, 2]. One of the new creative innovations of composite members is known as concrete-filled double skin steel tubes (CFDST), which represents the new generation of the concrete-filled steel tubes (CFST) composite members. CFDST, which was developed in the late 1980s [3], is made up of two concrete-filled concentric steel tubes. A CFDST column's inner and outer tubes may be made of a variety of materials to improve its appearance and resistance to corrosion [4]. Furthermore, CFDST columns may be constructed using a variety of steel tube profile types. The two most often utilised profile combinations are square hollow sections (SHS) and circular hollow sections (CHS), which are used as the inner and outer layers of the tube, respectively. Numerous research works have demonstrated that an increase in the bending stiffness, ductility, and fire resistant was observed when an inner steel tube is added to in steel-concrete composite columns [5-7]. In 2004, Han et al. [8] evaluated 14 steel tube specimens with various parameters, including the hollow phase percentage, the outer diameter of the tube, and the assist load's eccentricity, which were modified in the course of the experiments. The result showed that an improvement in strength and ductility for CFDST (CHS inner and SHS outer) stub columns, beams, and beam-columns was due to the "composite action" between the steel tubes and the sandwiched concrete. Also, they observed was a reasonable agreement achieved for All predictions were compared with test results. In 2006, Tao and Han [9] investigate the behaviour of CFDST beam columns with inner

and outer tubes made from rectangular hollow sections. Experiments were performed on three stub columns, three beams, and 24 beam-columns. A theoretical model for CFDST stub columns, beams, and beam-columns has been made, and simplified models have been made to estimate how much weight the composite specimens can hold. They found that CFDST members have a similar behaviour as the conventional CFST specimens. Additionally, increased strength and ductility have been reported for FDST (RHS inner and RHS outer) stub columns, beams, and beam-columns related to the "composite action" between the steel tube and the concrete core. Good agreement has been obtained between the predicted and experimental curves. Another study in 2010, by Han et al. [10] suggested a nonlinear concrete model for the analysis of DSCT columns. The suggested nonlinear concrete model discusses the reason a DSCT column exhibits superior strength higher than the average strengths of its component elements: an inner tube, an outside tube, and unconfined concrete. The strength is attributed to the inner tube not failing prior to the yield failure of the outer tube, which causes the concrete within the DSCT column to be contained triaxially until the column ultimately collapses. The confined concrete exhibits significantly more strength than unconfined concrete. In 2012, Dong and Ho [11] assessed the uniaxial behaviour of concrete-filled double-skin tubular (CFDST) columns with external steel rings, particularly in terms of strength and stiffness. The measured load-displacement curves, Poisson's ratio, axial strength, and stiffness for these columns were subsequently compared with those of CFDST columns without external confinement. It has been demonstrated that ring-confined CFDST columns are better than unconfined CFDST columns in strength, stiffness, and ductility. It is because the steel rings provide a more effective, uniform, and continuous confining pressure to the concrete core. In 2016, Aziz et al. [7] studied full-scale CFDST with variations in the thickness of the outer tube and the percentage of void fraction in terms of stress and strain relationships. The tested specimens made of self-compacting concrete (SCC) as mortar. From these results, it has been established that with an increased thickness of the outer shell, there is improved axial load-bearing capacity because the resistance is high due to increased pressure within the shell. Also, the experimental program applied proved that the failure mechanism of the CFDST column is based on the failure of the outer tube attributed to a combination of axial load and concrete expansion. In 2018, Saleh and Majeed [12], the efficacy of high-strength concrete double-walled tubular steel columns was studied. Fourteen different column shapes were evaluated in order to explore the effects of various parameters, including the shape of the column's cross section (round or square), the amount of space available for the void, the type of infill (normal or high strength), and the slenderness of the column. They found that the ultimate axial strength of square HSCFDST columns exceeds that of circular columns, while their sectional characteristics are essentially equivalent. Additionally, the ultimate axial strength of both the circular and square HSCFDST columns was inversely proportional to their hollowness and slenderness ratios.

The use of sustainable concrete in CFDST columns may develop an emerging research area in sustainable construction. This may lead to reducing the construction cost in such columns in addition to different environmental benefits. The primary ingredients of concrete are coarse aggregates, freshwater, and river sand. Concrete consumption has grown dramatically during the last ten years due to urbanisation, particularly the fast growth of coastal cities [13, 14]. Such high consumption can have a significant negative impact in terms of increasing the demand on non-renewable natural resources. In this regard, one reasonable approach is the use of sustainable and recyclable resources in construction applications. The use of materials such as recycled aggregate (RA) in concrete construction may benefit both the environment and the building industry [15]. In the field of concrete technology, utilising recycled aggregates (RA) in concrete, instead of natural aggregates (NA), can not only be effective in minimising the demand for natural resources but also in solving the issue of waste concrete pollution. Since the past two decades, efforts to exploit RA in concrete construction have been carried out, and considerable research has been conducted in this regard. In 2006, Yang and Han [16] investigated the effect of RAC on the efficiency of circular and square CFST columns. The present research tested thirty concrete-filled tube composite columns, including 24 RAC-FST columns and 6 NAC-FST columns. The main variables investigated in this study included section shape, type of concrete (natural concrete and concrete including recycled aggregates), and the load eccentricity ratio, which ranged from zero to 0.5. In concrete manufacturing, 25% and 50% recycled aggregate (RA) were used as substitutes for natural coarse aggregate, employing three distinct concrete mix types to construct the test specimens. The researchers observed that almost all of the test specimens had ductile behavior. The ultimate strength of specimens incorporating RAC was a little lower than that for those filled with normal concrete; however, they exhibited comparable compressive properties and similar behaviour. Similar findings were also observed in [16-19]. Another study in 2020 by Yu et al. [20] observed that, with a higher replacement ratio of RA as well as the  $D/t$  ratio of the steel tube, all specimens' bearing capacity dropped, while peak loads for the specimens tended to increase as concrete strength grade increased. In 2021, Liu et al. [21] investigated several methods to improve the adhesive characteristics between recycled aggregate concrete and steel tubes. These methods include the incorporation of steel fibres, modifications to the water-to-binder ratio, and conventional strategies such as thickening steel tubes. The research results indicated that replacing natural concrete with recycled aggregate (RA) led to a reduction in bond strength of about 25.06 % and increased the degradation rate, attributed to the early development and exacerbation of cracks. In 2021, Wu et al. [22] observed that the peak load of the specimens exhibited a decrease-rise-decrease behaviour as the RA replacement ratio increased, varying between 76% and 122%.

It can be seen from the abovementioned research studies that very few experimental studies have investigated the structural behaviour of concrete-filled double-skin steel tubular columns. More specifically, most of the reviewed research has primarily emphasised the structural performance of normal concrete (NC) rather than self-compacting concrete (SCC). Therefore, further experimental investigations in this area are necessary. In this study, the aim was to investigate the influence of recycled aggregate on the structural behaviour of SCC CFDST columns made with varying inner and outer tube shapes, distances, manufactured materials, and replacement percentages of RA. The percentage replacements of RA, 0%, 30%, and 60%, were used. A series of rectangular and circular reinforced SCC CFDST columns were prepared and

tested until failure. The performance of the tested beams was assessed in terms of cracking load, load–deflection response, ultimate failure load, and crack morphology.

## 2. Experimental work

In this work, ten CFDST simply supported columns were tested. Normal strength (NS) concrete columns were designed and produced for studying the influence of recycled aggregate replacement ratio and hollowness ratio in SCC columns until failure. Nine CFDST column specimens were made from hot-rolled steel sections, except for one specimen, which was made from cold-formed steel sections to make the comparison. Thus, three different ratios, namely 0%, 30%, and 60%, were used in the replacement of recycled aggregate. Based on the shape of their inner steel tubes, we categorised the tested column specimens into three groups. The first group of the columns has a square ( $150 \times 150 \times 4$  mm) outer tube and inner tube ( $100 \times 100$  mm) made with three different percentages (0%, 30%, and 60%) of recycled aggregate. This group begins with the name of the specimens (SS1). The second group consists of three columns with a square inner tube with dimensions ( $75 \times 75 \times 2$  mm). This group begins with the name of the specimens (SS2). Finally, the third group comprises three columns, each featuring a circular inner tube with dimensions ranging from 75 to 2 mm. The name of the specimens in this group begins with SC1. Another set of tested column specimens made from cold-formed steel tubes was used to look at how the columns themselves affected the behaviour of CFDST columns. To ensure that the cross-sectional area of the members is approximately equal, this specimen is made up of a square outer tube of dimensions  $150 \text{ mm} \times 150 \text{ mm} \times 3$  mm. The replacement ratio of RCA was kept at 30%. The designation of the tested specimens is present in Table 1.

**Table 1:** Identification of the tested CFDST columns

| Column designation | Column details                                                                   |
|--------------------|----------------------------------------------------------------------------------|
| SS1-R00            | Square outer tube– Square inner tube– 0% recycled aggregate (Reference columns)  |
| SS1-R30            | Square outer tube– Square inner tube– 30% recycled aggregate                     |
| SS1-R60            | Square outer tube– Square inner tube– 60% recycled aggregate                     |
| SS2-R00            | Square outer tube– Square inner tube– 0% recycled aggregate (Reference columns)  |
| SS2-R30            | Square outer tube– Square inner tube– 30% recycled aggregate                     |
| SS2-R60            | Square outer tube– Square inner tube– 30% recycled aggregate                     |
| SC2-R00            | Square outer tube– Square inner tube– 30% recycled aggregate                     |
| SC2-R30            | Square outer tube– Circle inner tube– 30% recycled aggregate (Reference columns) |
| SC2-R60            | Square outer tube– Circle inner tube– 60% recycled aggregate (Reference columns) |
| SS2-R30C           | Square outer tube– Square inner tube– 30% recycled aggregate– Cold form          |

### 2.1. Geometrical properties and reinforcement details

In this experimental study, nine CFDST hot-formed column specimens were available in the local markets at a fixed length of 6 m and were tested. The specimens were cut uniformly to a length of 0.8 m for all sections and bevelled to ensure that the height of all column specimens, as indicated in Figure 1, was set at 780 mm. As shown in Figures 1 and Table 2, all specimens were made with a steel thickness of 4 mm per outer steel layer and 2 mm per inner steel layer. All square columns have the same external dimension of the cross-section, the outer steel tubes, and the variety of inner dimensions of the cross-section. The external dimensions were  $150 \text{ mm} \times 150 \text{ mm}$  for the outer tubes. The column specimens were bottom-supported during casting by providing a temporary base to fix them, thereby maintaining the centrality of the columns, as in Figure 1. The tested specimens were subjected to axial point loads up to failure. Figure 2 shows details of the test column specimens in the study.

**Table 2:** Details of Tested CFDST columns

| Column Name | Outer Steel Section |                |                | Inner Steel Section |                |                | Recycle Aggregate Ratio (%) |
|-------------|---------------------|----------------|----------------|---------------------|----------------|----------------|-----------------------------|
|             | Shape               | Dimension (mm) | Thickness (mm) | Shape               | Dimension (mm) | Thickness (mm) |                             |
| SS1-R00     | Square              | 150            | 4              | Square              | 100            | 2              | 0                           |
| SS1-R30     | Square              | 150            | 4              | Square              | 100            | 2              | 30                          |
| SS1-R60     | Square              | 150            | 4              | Square              | 100            | 2              | 60                          |
| SS2-R00     | Square              | 150            | 4              | Square              | 75             | 2              | 0                           |
| SS2-R30     | Square              | 150            | 4              | Square              | 75             | 2              | 30                          |
| SS2-R60     | Square              | 150            | 4              | Square              | 75             | 2              | 60                          |
| SC2-R00     | Square              | 150            | 4              | Circle              | 75             | 2              | 0                           |
| SC2-R30     | Square              | 150            | 4              | Circle              | 75             | 2              | 30                          |
| SC2-R60     | Square              | 150            | 4              | Circle              | 75             | 2              | 60                          |
| SS2-R30C    | Square              | 146            | 3              | Square              | 75             | 2              | 30                          |

\*The symbol name with c letter in the end are the cold form steel section



**Fig. 1:** Preparation CFDST columns.

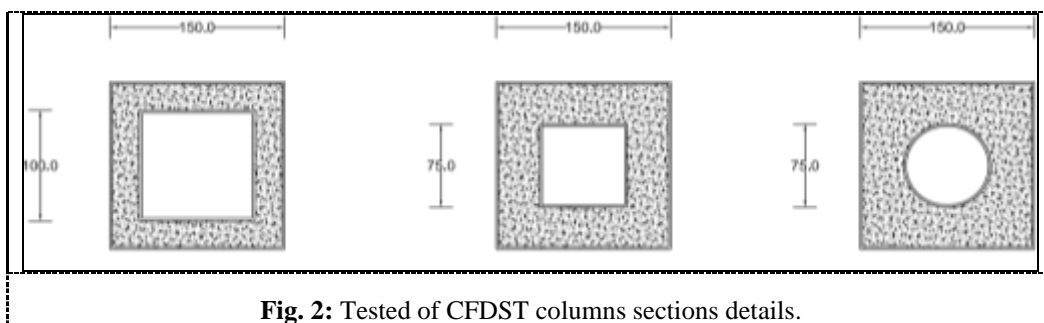


**Fig. 2:** Tested of CFDST columns sections details.

## 2.2. Materials

### 2.2.1. Binders

Locally ordinary Portland cement type I met the requirements of the Iraqi Specification (IQS) [23] was used. Ordinary Portland cement type I, satisfied with the Iraqi Requirement (IQS) [23], was utilised. Limestone powder (LP) that was less than 0.125 mm was used to increase the amount of fine materials, which in turn increases the mix's fluidity and consistency, as well as its resistance to segregation, which satisfies the EFNARC guidelines (EFNARC, 2005) [24]. Table 3 shows the chemical composition of the limestone powder used.

**Table 3:** Chemical composition of the limestone powder.

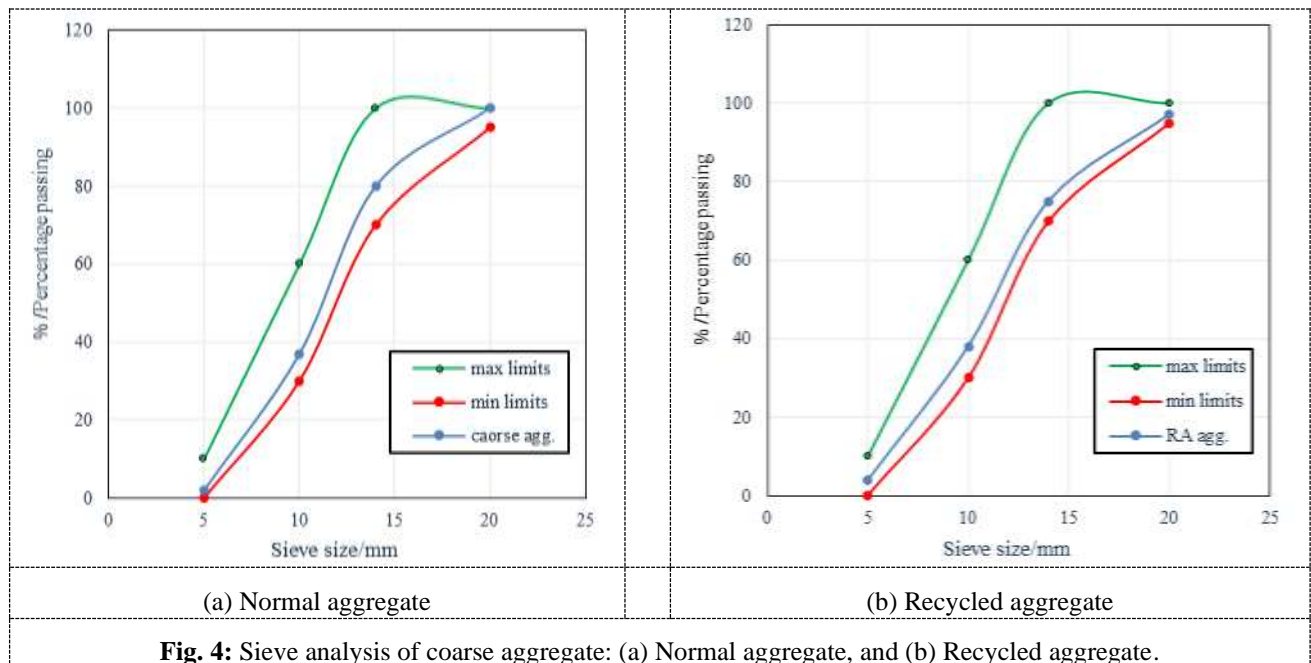
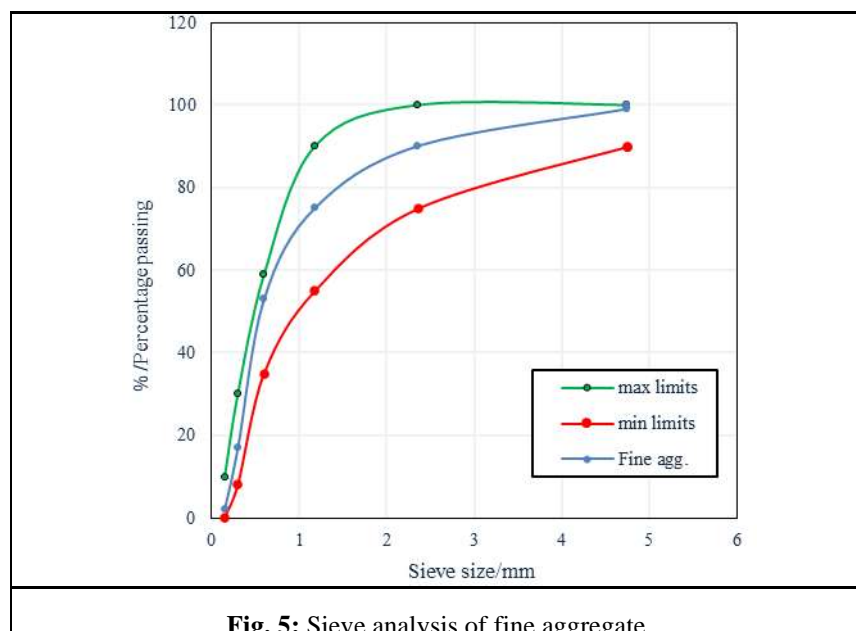
| Chemical Composition           | Content % |
|--------------------------------|-----------|
| SiO <sub>2</sub>               | 1.38      |
| Fe <sub>2</sub> O <sub>3</sub> | 0.12      |
| Al <sub>2</sub> O <sub>3</sub> | 0.72      |
| CaCO <sub>3</sub>              | 88.5      |
| MgO                            | 0.13      |
| SO <sub>3</sub>                | 0.21      |
| L.O.I                          | 3.94      |

### 2.2.2. Aggregate

Two types of coarse aggregates, NA and RA, with a maximum size of 20 mm were used (Tables 4). RA was obtained from crushing concrete cubes previously tested in the construction laboratory of The Engineering College et Al-University of Basra. The average strength of these cubes was between 25–30 MPa. The specimens and crushing process are present in Figure 3. The physical properties of NA and RA aggregate were tested at the Structural Laboratory of the Engineering Consulting Office at the College of Engineering, Basra University. The results are shown in Table 4. Both aggregates met the Iraqi specifications, Standard No. [25] (45/1984), as in Table 4. All aggregate was used in saturated surface dry conditions (S.S.D). Figure (5-3) presents the sieve analysis of this aggregate. Table 4 shows the specific gravity and absorption of recycled concrete. Further, a locally available sand with a maximum size of 4.75 mm was used as fine aggregate in this investigation (Figure 4). Fine aggregates satisfy the IQS [26]. Figure 5 shows the sieve analysis of fine aggregate. Normal sand with a volume of 0.6 mm, a specific gravity of 2.65, a sulphate content of 0.33%, an absorption rate of 1.1%, and Loose bulk density of 1645 kg/m<sup>3</sup> was used. It was used in saturated surface dry conditions (S.S.D.).

**Table 4:** Physical Properties of the NA and RCA.

| Physical properties                  | NA      | RA      | Limits of IOS<br>No.45/1984 [25] |
|--------------------------------------|---------|---------|----------------------------------|
| Specific gravity                     | 2.65    | 2.33    | --                               |
| Sulfate content (SO <sub>3</sub> )   | 0.073 % | 0.08 %  | ≤ 0.1 %                          |
| Chloride content (Cl)                | 0.092 % | 0.053 % | ≤ 0.1 %                          |
| Absorption                           | 0.65 %  | 0.65 %  | --                               |
| Loose bulk density kg/m <sup>3</sup> | 1500    | 2034    | --                               |

**Fig. 3:** Recycled aggregate preparation.**Fig. 4:** Sieve analysis of coarse aggregate: (a) Normal aggregate, and (b) Recycled aggregate.



### 2.2.3. Superplasticizer

The Platinum PC 8200 was used as a superplasticizer (SP) in this investigation. It satisfies the ASTM C-494 type F specification. Table 5 and Appendix A show the properties of the used SP and the data product sheet, respectively.

**Table 5:** Technical data of Platinum PC 8200 superplasticizer

| Property                  | Description                                  |
|---------------------------|----------------------------------------------|
| Color, Appearance         | Amber liquid                                 |
| pH                        | 3-7                                          |
| Density                   | $1.08 \pm 0.02 \text{ g/cm}^3$               |
| Chlorine Content (%)      | < 0,1 (EN 480-10)                            |
| Alkaline Content (%)      | < 10 (EN 480-12)                             |
| Compliance with Standards | ASTM C 494 Type F EN 934-2 Table 3.1 and 3.2 |

### 2.2.4. Steel tubular

The hot-rolled and cold-formed round and square hollow tubes were used in this work. To calculate the mechanical properties of the steel beams, the Computer Numerical Control (CNC) machine cut three tension dog bones (steel tubes) from the web (Figure 6). Table 6 below shows the tensile test results of the hot-rolled and cold-rolled steel materials used in the current experiments. The dog bones conform to ASTM A 36/A 36M standards [27]. For testing the dog bone samples, a universal testing machine was available in the Structural Laboratory of the Civil Engineering Department at Basra University (Figure 6).

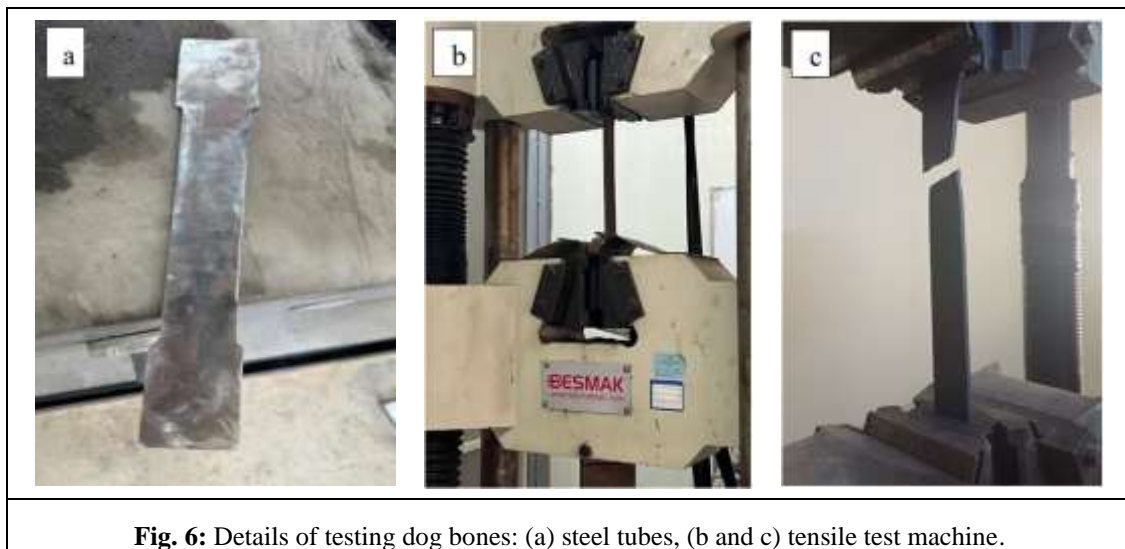


**Fig. 6:** Details of testing dog bones: (a) steel tubes, (b and c) tensile test machine.

| Item                                   | Circular Steel Tube | Square Steel Tube | Average Value (MPa) | ASTM A 36/A 36M Requirements [27] |
|----------------------------------------|---------------------|-------------------|---------------------|-----------------------------------|
| Yield stress(N/mm <sup>2</sup> )       | 341                 | 338               | 340                 | 250 Minim                         |
| Ultimate Strength (N/mm <sup>2</sup> ) | 482                 | 482               | 482                 | 400-550                           |

## 3. Mix proportion

An experimental work was dedicated on producing a series of SCC mixes with a nominal compressive strength of 30 MPa at 28-days (i.e. w/c ratio of 0.43 and 0.48). The designed using the rational and straightforward mix proportioning method proposed in ACI 237R-07 [28]. In the preparation of the SCC mixes, two types of coarse aggregates (NA and RA), in saturated surface dry conditions, were utilised. The replacement of NA by RA was volumetrically implemented based on their specific gravities in order to keep the other amounts of mix ingredients without adjustment. The mixed ingredients of all investigated mixes are presented in Table 7.

**Table 7:** Constituent materials of the prepared concrete mixes, kg/m<sup>3</sup>

| Mix type | w/c  | Cement | Water | LP  | super-plasticizers | Fine aggregate | RA aggregate | Coarse aggregate |
|----------|------|--------|-------|-----|--------------------|----------------|--------------|------------------|
| SCC-0RA  | 0.48 | 315    | 181   | 151 | 0.85               | 755            | 0            | 944              |
| SCC-30RA | 0.43 | 290    | 163   | 124 | 0.76               | 646            | 264          | 320              |
| SCC-60RA | 0.43 | 290    | 160   | 124 | 0.76               | 646            | 492          | 320              |

#### 4. Concrete columns specimens casting and curing

Ten CFDST specimens were fabricated in the present study. Nine of them were made from hot-rolled steel tubular sections, and one column was made from cold-rolled steel tubular sections. Before the casting process, a piece of steel rod was used to hold the outer and inner steel tubes of each specimen in place from the bottom and the top. This was done to make sure that the tubes would be straight when concrete was poured inside them (see figure 7). Figure 8 describes the construction of the column specimens. For casting specimens, a vertical portable mixer with a capacity of 0.2 m<sup>3</sup> was used for mixing fresh SCC. After that, the column samples were cast, and the models' top surfaces were adjusted. To evaluate the experimental mechanical properties of the cast mix, we cast cube and cylinder specimens for every beam specimen. Following that, the samples were kept in a laboratory environment and covered to maintain them in a humid environment. Figure 8 shows the mixing, casting, and curing of the specimens.

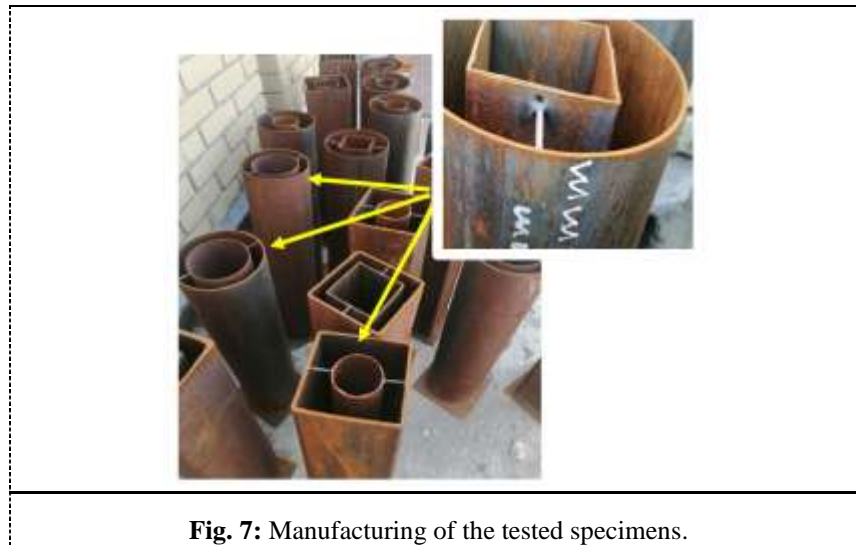


**Fig. 7:** Manufacturing of the tested specimens.

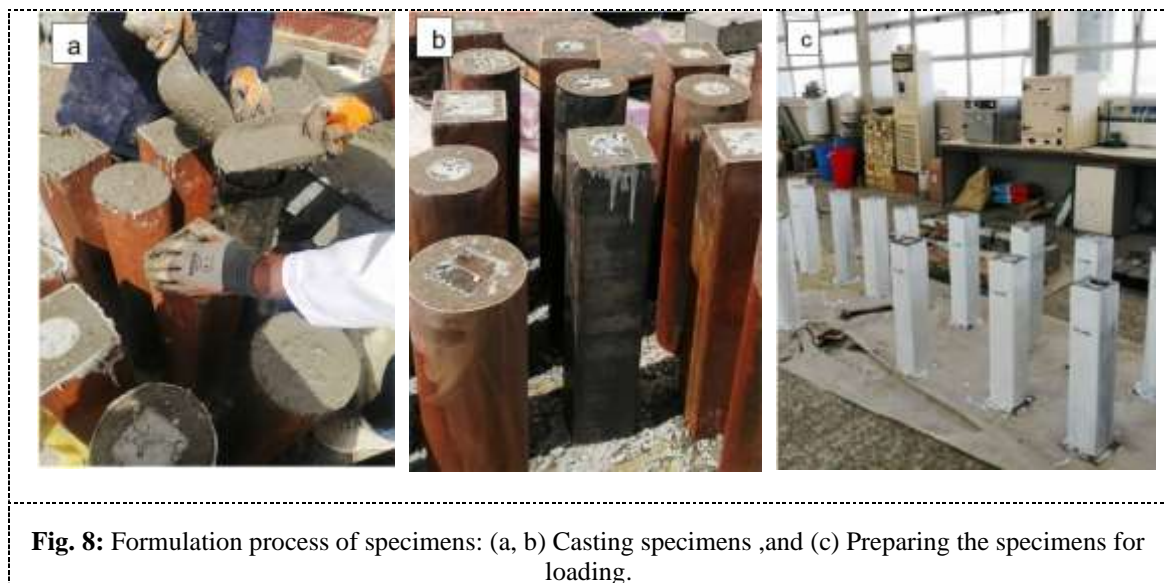


**Fig. 8:** Formulation process of specimens: (a, b) Casting specimens ,and (c) Preparing the specimens for loading.

#### 5. Test setup and instrumentation

A universal testing instrument with a maximum capacity of 200 Ton was utilised for testing the column specimens under eccentric loading condition (Figure 9). The device was obtainable in the Structural Laboratory of the Civil Engineering Department at Basra University. As illustrated in Figure 10, the tested CFDST columns had been painted two days prior to testing for easier observation of the developed and propagated cracks. A laser linear variable differential transducer (LVDT) was employed to measure the deflection at the middle length of the columns due to the applied load (Figure 11). During the test, a steel plate is put on top of each column specimen to spread the load during compression and make sure the laser reading is correct, as seen in Figure 11. The load is then applied at a low level of rating to ensure correct representation of the nature of static loading. The failure mode, load versus axial displacement, and the ultimate capacity of each column specimen were recorded during the test, where all the readings were taken until the specimens reached the failure stage.



**Fig. 9:** The used hydraulic testing machine.



**Fig. 10:** Installation of the laser LVDT device.



**Fig. 11:** Laser device reading.

## 6. Result and discussion

Ten reinforced sustainable CFDST columns made with SCC core were prepared to investigate their structural behavior. Nine columns, which were made of hot-rolled steel sections, were tested until failure, while the others were made from cold-formed CFDST. Table 8 summarises the experimental test results for the column specimens, including their ultimate capacity, failure load, and failure mode. The following sections discuss and evaluate the results along with the load-displacement curves.

**Table 8:** Experimental results for the tested CFDST columns

| No. | Column designation | RAC (%) | Ultimate capacity (kN) | Failure load increase over Control Column* (%) | $\Delta_{max}$ (mm) | Ratio relative to the control Column* | Failure mode   |
|-----|--------------------|---------|------------------------|------------------------------------------------|---------------------|---------------------------------------|----------------|
| 1   | SS1-R00            | 0       | 1400                   | --                                             | 5.0                 | --                                    | Local buckling |
| 2   | SS1-R30            | 30      | 1250                   | -10.7                                          | 3.9                 | -22.0                                 | Local buckling |
| 3   | SS1-R60            | 60      | 1240                   | -11.4                                          | 6.5                 | +30.0                                 | Local buckling |
| 4   | SS2-R00            | 0       | 1420                   | --                                             | 7.3                 | --                                    | Local buckling |
| 5   | SS2-R30            | 30      | 1395                   | -1.8                                           | 3.3                 | -54.8                                 | Local buckling |
| 6   | SS2-R60            | 60      | 1260                   | -11.3                                          | 11.2                | -53.4                                 | Local buckling |
| 7   | SC2-R00            | 0       | 1460                   | --                                             | 7.4                 | --                                    | Local buckling |
| 8   | SC2-R30            | 30      | 1400                   | -4.1                                           | 9.2                 | +24.3                                 | Local buckling |
| 9   | SC2-R60            | 60      | 1350                   | -7.5                                           | 9.3                 | +25.7                                 | Local buckling |
| 10  | SS2-R30C           | 30      | 800                    | -11.1                                          | 6.4                 | --                                    | Local buckling |

\*This is the ratio of the ultimate load of columns relative to the control column with natural aggregate (0% RA replacement), (+) means increase (%) in the above properties with respect to reference column, (-) means decrease (%) in the above properties.

### 6.1. Effect of hollowness ratio and shape

#### 6.1.1. Square CFDST columns with 0% RA

Three CFDST columns that were previously mentioned, which were produced with normal aggregate (0% recycled aggregate). When comparing the experimental results of this group of the CFDST specimens [SS1-R00, SS2-R00, and SC2-R00], which were tested under axial loading, it can be noted that local buckling failure occurred for these tested specimens. Table 9 and Figure 12 present the experimental outcomes of these tested column specimens. It can be shown that the maximum load capacity of the control column SS1-R00 is 1400 kN, with a corresponding displacement of 5 mm. Further, it can be seen that the stiffness of the SC2-R00 and SS2-R00 columns, respectively, was higher than reference column. The maximum load capacity of the SC2-R00 and SS2-R00 specimens is 1460 and 1420 kN, which is about +4.29% and +1.43% higher than the control columns (SS1-R00 columns), with a corresponding displacement of 7.4 and 7.3 mm, respectively. The control column (SS1-R00) features a square inner tube of 100 mm by 100 mm and possesses a hollowness ratio of 0.704. A comparison with the column (SS2-R00), which features a square tube (75×75 mm) and a hollowness ratio (0.528), revealed an enhancement in maximum bearing capacity. Also, a comparison between the column (SS2-R00) with a square inner tube (75×75 mm) and the column (SC2-R00) with a circular inner tube (75 mm diameter) indicates that an increase in strength was noted for the circular inner section although the hollowness ratio between the two columns is same as shown in Table (4.3), signifying that the Fixed hollowness ratio with shape change influences on the maximum load capacity. Figure 13 illustrates the failure mode of square CFDST columns made with normal aggregate and containing square or circular inner sections. It can be observed that the concentrically loaded columns showed local buckling without and crushing of concrete core in all the three specimens. The affected regions are located at the top and/or lower ends nearest to the loading plates, as seen in Figure 13. This was predicted according to the uniformly distributed compression forces along the whole column section. Results from studies indicate that the inner tube offers substantial



support to the sandwich concrete, and the performance of the composite member resembles that of the concrete-filled steel tube [29].

**Table 9:** Experimental results for the tested Square CFDST Columns with 0% RA.

| No. | Column designation | RAC (%) | Ultimate capacity (kN) | Failure load increase over Control Column* (%) | $\Delta_{max}$ (mm) | Ratio relative to the control Column* | Failure mode   |
|-----|--------------------|---------|------------------------|------------------------------------------------|---------------------|---------------------------------------|----------------|
| 1   | SS1-R00            | 0       | 1400                   | --                                             | 5                   | --                                    | Local buckling |
| 2   | SS2-R00            | 0       | 1420                   | +1.43%                                         | 7.3                 | +46%                                  | Local buckling |
| 3   | SC2-R00            | 0       | 1460                   | +4.29%                                         | 7.4                 | +48%                                  | Local buckling |

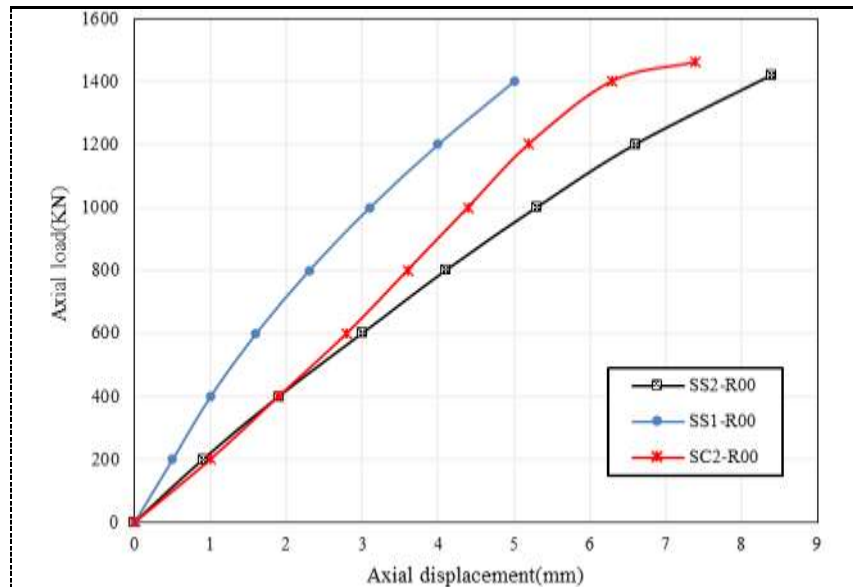


**Fig. 12:** Load- deflection response for square columns of 0%RA.



**Fig. 13:** Failure mechanisms for square-tested columns with axial loading made with 0%RA.

### 6.1.2. Square CFDST columns with 30% RA

In this group, three CFDST columns were previously mentioned, which were produced with recycled aggregate (30% recycled aggregate). When comparing the experimental results of this group of the CFDST specimens [SS1-R30, SS2-R30, and SC2-R30], which were tested under axial loading, it can be noted that local buckling failure occurred for these tested specimens. Table 10 and Figure 14 present the experimental outcomes of the tested column specimens. As the inner wall dimensions decrease, the displacements under peak loads of the CDFST columns increase. In the figure, it can be observed that the CFDST specimens with circular inner confinement performed better in terms of strength, stiffness, and ductility than those with square inner confinement. The maximum load capacity of the control column SS1-R30 is 1250 kN, with a corresponding displacement of 3.9 mm (figure 14 and Table 10). Also, it can be seen that the maximum load capacity of the SC2-R30 and SS2-R30 specimens is 1400 and 1395 kN, which is about 12% and 11.6% higher than the column (SS1-R30 column), with a corresponding displacement of 9.2 and 3.3 mm, respectively. When compared the control column (SS1-R30) that has a square inner tube of 100 mm by 100 mm and a hollowness ratio of 0.704, the column (SS2-R30), which incorporates a square tube (75×75 mm) with a hollowness ratio of 0.528, demonstrated an improvement in maximum bearing capacity about 11.6%. Furthermore, a juxtaposition of the column (SS2-R30) featuring a square inner tube (75×75

mm) and the column (SC2-R30) with a circular inner tube (75 mm diameter) revealed a notable increase in strength for the circular inner section. Despite the equal hollowness ratio between the two columns, as indicated in Table 10, This means that the hollowness ratio combined with the circular shape of the inner tube gives a greater improvement in the maximum load capacity Compared to the same hollowness ratio of tube to square in spite of the use of different concrete (where in this case, a concrete core with 30% RA). The failure modes of the columns are illustrated in Figures 15. All the tested columns with concentric loads exhibited local buckling. The expected failure mode of a column is the compression crushing of the concrete combined with the yielding of the steel. Nevertheless, the properties of the outer and inner steel tubes, and the compressive strength of the concrete affected the failure behavior. It is essential to point out that the columns exhibited significant lateral deformations characterized by local buckling. Moreover, the concrete in those columns failed, which can be demonstrated by the performance percentage of recycled aggregate. This behavior can be noted in the failure modes of SC2-R30 column made with a circular inner section. On the other hand, most of the specimens (SS1-30RA and SS2-30RA specimens), which have square inner section tubes, exhibited compression-dominant failure, and the lateral deformations in these columns are less visible.

**Table 10:** Experimental results for the tested Square CFDST Columns with 30% RA

| No. | Column designation | RAC (%) | Ultimate capacity (kN) | Failure load increase over Control Column* (%) | $\Delta_{max}$ (mm) | Ratio relative to the control Column* | Failure mode   |
|-----|--------------------|---------|------------------------|------------------------------------------------|---------------------|---------------------------------------|----------------|
| 1   | SS1-R30            | 30      | 1250                   | --                                             | 3.9                 | --                                    | Local buckling |
| 2   | SS2-R30            | 30      | 1395                   | +11.6%                                         | 3.3                 | -15.38%                               | Local buckling |
| 3   | SC2-R30            | 30      | 1400                   | +12%                                           | 9.2                 | +135.9%                               | Local buckling |

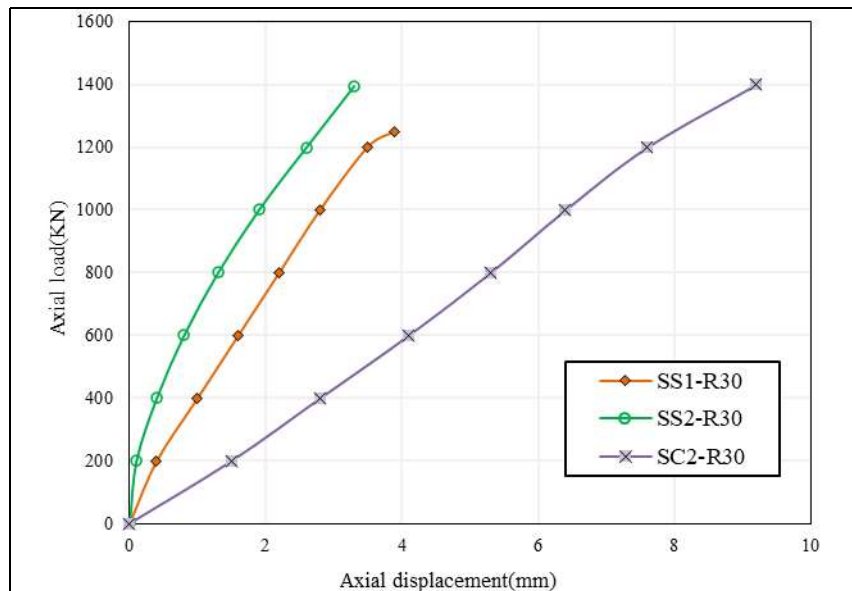


**Fig. 14:** Load- deflection response for square columns of 30%RA.



**Fig. 15:** Failure modes for square-tested columns with axial loading made with 30%RA.

### 6.1.3. Square CFDST columns with 60% RA

In this group, three CFDST columns were previously mentioned, which were produced with recycled aggregate (60% recycled aggregate). When comparing the experimental results of this group of the CFDST specimens [SS1-R60, SS2-R60, and SC2-R60], which were tested under axial loading, it can be noted that local buckling failure occurred for these tested specimens. Table 11 and Figure 16 present the experimental outcomes of the tested column specimens. The maximum load capacity of the control column SS1-R60 is 1240 kN, with a corresponding displacement of 6.5 mm (Figure 16 and Table 11). On the other hand, SS2-R60 columns developed higher ductile behavior than the SC2-R60, and control specimen. The maximum load capacity of the SC2-R60 and SS2-R60 specimens is 1350 and 1260 kN, which is about 8.9% and 1.61% higher than the control columns (SS1-R60 columns), with a corresponding displacement of 9.3 and 11.2 mm, respectively. The degradations in compression capacity of the specimens SS1-R60 and SS2-R60 could be attributed to the characteristics of the inner tube. The SS1-R60 control column has a 100mm side length square inner tube with a 0.704 hollowness ratio. The maximum bearing capacity was found to be higher in the column (SS2-R60) with its square inner tube 75mm side length and hollowness ratio of 0.528. Also, in comparing the results of column (SS2-R60) and (SC2-R60), it was also found that the column (SC2-R60) with inner circular tube is better in terms of endurance of the maximum applied force as shown in Table 11.

It is crucial to capture that in the specimens that square outer tubes, the failure paths are accompanied by outward local buckling of the tubes. In addition, there is no signs for the happiness of concrete crushing. However, it was noted that the volume of the buckling region is relatively higher than that noted in the tested CFDST columns with 30% RA, and the in those columns is greater than that the specimens with 0% RA.

**Table 11:** Experimental results for the tested square CFDST columns with 60% RA

| No. | Column designation | RAC (%) | Ultimate capacity (kN) | Failure load increase over Control Column* (%) | $\Delta_{max}$ (mm) | Ratio relative to the control Column* | Failure mode   |
|-----|--------------------|---------|------------------------|------------------------------------------------|---------------------|---------------------------------------|----------------|
| 1   | SS1-R60            | 60      | 1240                   | --                                             | 6.5                 | --                                    | Local buckling |
| 2   | SS2-R60            | 60      | 1260                   | +1.61%                                         | 11.2                | +72.3%                                | Local buckling |
| 3   | SC2-R60            | 60      | 1350                   | +8.9%                                          | 9.3                 | +43.1%                                | Local buckling |

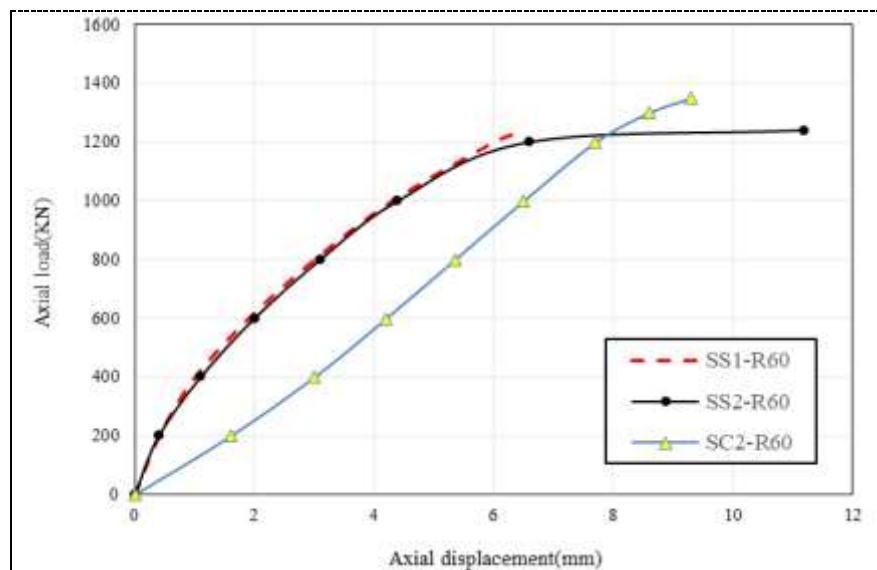


**Fig. 16:** Load- deflection response for square columns of 60% RA.



**Fig. 17:** Failure modes for square-tested columns with axial loading made with 60% RA.

## 6.2. Effect of replacement ratio of recycled aggregate

### 6.2.1. Square CFDST columns with 70% hollowness ratio

Three CFDST columns [SS1-R00, SS1-R30, and SS1-R60] were produced with (0%, 30%, 60%) recycled aggregate ratios for the samples mentioned above. When comparing the results for these tested column specimens under axial load, Figure 18 shows that the maximum load capacity for column (SS1-R00) is 1400 kN and it can also be noted that the stiffness of columns (SS1-R30 and SS1-R60) was 1250 and 1240 kN respectively, and they are less than the control column (SS1-R00) at the ratios 10.74% and 11.43%, respectively, as shown in Table 12. These reductions are happened in spite of that the three specimens have approximately the same properties except the use RA ratio.

**Table 12:** Experimental results for the tested Square CFDST columns with 70% hollowness ratio

| No. | Column designation | RAC (%) | Ultimate capacity (kN) | Failure load increase over Control Column* (%) | $\Delta_{max}$ (mm) | Ratio relative to the control Column* | Failure mode   |
|-----|--------------------|---------|------------------------|------------------------------------------------|---------------------|---------------------------------------|----------------|
| 1   | SS1-R00            | 0       | 1400                   | --                                             | 5                   | --                                    | Local buckling |
| 2   | SS1-R30            | 30      | 1250                   | -10.74%                                        | 3.9                 | -22%                                  | Local buckling |
| 3   | SS1-R60            | 60      | 1240                   | -11.43%                                        | 6.5                 | +30%                                  | Local buckling |

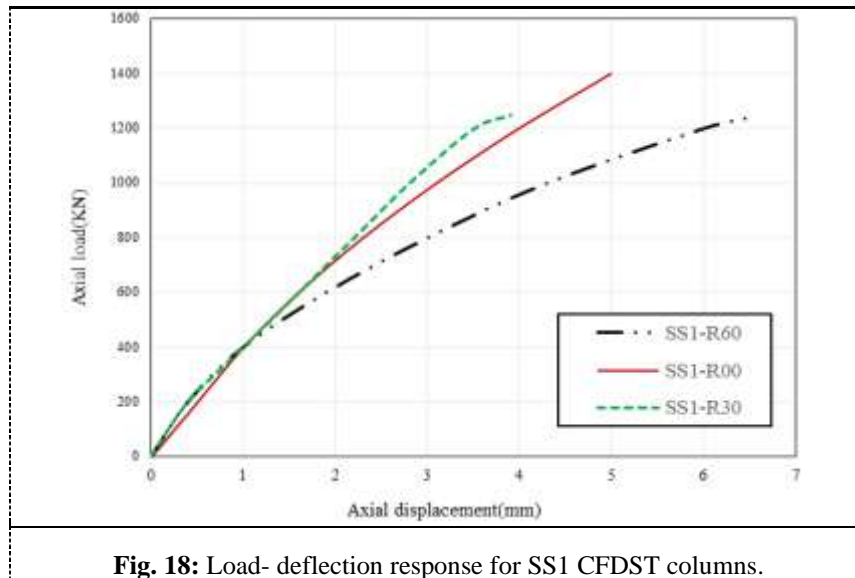


**Fig. 18:** Load- deflection response for SS1 CFDST columns.

### 6.2.2. Square CFDST columns with 53% hollowness ratio

Experimental results of these samples [SS2-R00, SS2-R30, and SS2-R60] It can be noted that the Table 13 and the Figure 19 show the experimental results of these columns, where it was noted that the specimen (SS2-R00) with zero replacement ratio of RA is also give better performance, stiffness and high strength than those with higher replacement ratios of RA in spite of the hollowness ratio of these columns is lesser than the last ones. The maximum load capacity of column (SS2-R00) is higher than (SS2-R30). It is also noted that column (SS2-R60) has the lowest load capacity among the group, which was about 1260 kN.

On the other hand, the square column specimens that fabricated with the same hollowness ratio but with a circular shape [SC2-R00, SC2-R30, and SC2-R60], developed a batter ultimate capacity comparing with those having the same hollowness ratio but with a square inner tube [SS2-R00, SS2-R30, and SS2-R60]. Table 13 and Figure 20 present the experimental outcomes of the tested column specimens. The control specimen (SC2-R00) exhibited a high ultimate loading capacity shown in Table 13. The maximum load capacity of the control column SC2-R00 is (1460) kN. On the other hand, SC2-R60 column developed lower load capacity behavior than the SC2-R30 specimen. The maximum load capacity of the SC2-R30 and SC2-R60 specimens is 1400kN and 1350kN, which is about 4.11% and 7.53% lower than the control columns (SC2-R00 column).

**Table 13:** Experimental results for the tested Square CFDST columns with 53% hollowness ratio

| No. | Column designation | RAC (%) | Ultimate capacity (kN) | Failure load increase over Control Column* (%) | $\Delta_{max}$ (mm) | Ratio relative to the control Column* | Failure mode   |
|-----|--------------------|---------|------------------------|------------------------------------------------|---------------------|---------------------------------------|----------------|
| 1   | SS2-R00            | 0       | 1420                   | --                                             | 7.3                 | --                                    | Local buckling |
| 2   | SS2-R30            | 30      | 1395                   | -1.76%                                         | 3.3                 | -54.79%                               | Local buckling |
| 3   | SS2-R60            | 60      | 1260                   | -11.27%                                        | 11.2                | -53.4%                                | Local buckling |
| 4   | SC2-R00            | 0       | 1460                   | --                                             | 7.4                 | --                                    | Local buckling |
| 5   | SC2-R30            | 30      | 1400                   | -4.11%                                         | 9.2                 | +24.32%                               | Local buckling |
| 6   | SC2-R60            | 60      | 1350                   | -7.53%                                         | 9.3                 | +25.67%                               | Local buckling |



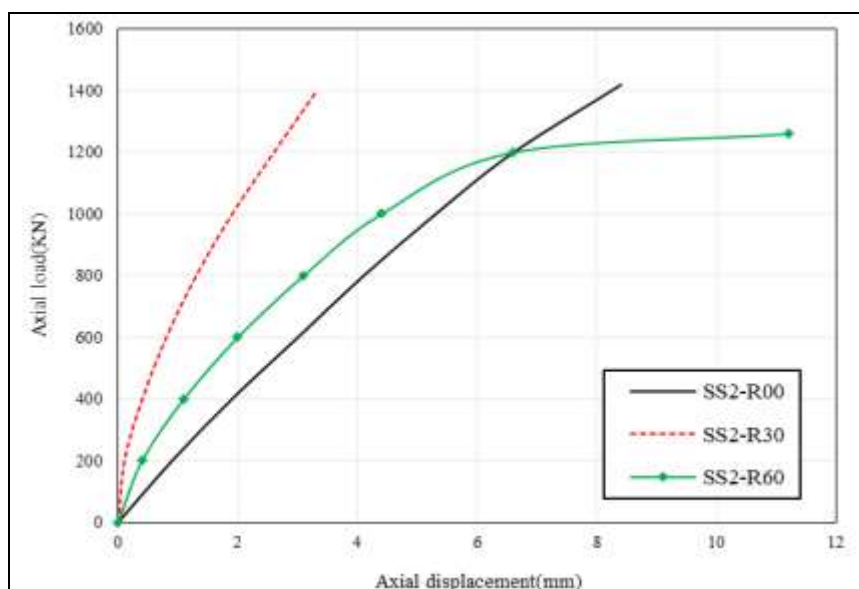


**Fig. 19:** Load- deflection response for SS2 CFDST columns.

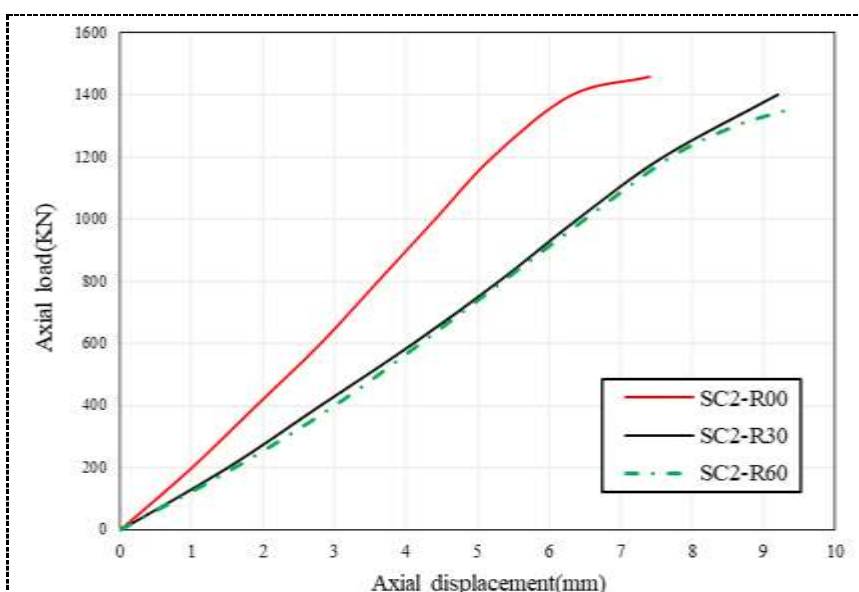


**Fig. 20:** Load- deflection response for SC2 CFDST columns.

## 7. Mathematical analysis of tested CFDST columns

The analytically predicted ultimate axial strength values of the experimentally investigated CFDST column specimens was evaluated and compared with the experimental ones. The analytical approach for the analysis of CFDST columns that described in chapter one was adopted to evaluate the analytical axial capacity of the tested CFDST column for a comparison. It was found that the results of both approaches are very close with a mean value of the ratio ( $P_{exp} / P_{anal}$ ) equal to about 1.14, 1.14, and 1.12 with 0%, 30% and 60% of RA replacement in the column specimens. Also, it can be noted that the analytical results were almost lower compared to that of the experimental results.

**Table 14:** Comparison of analytical results with tested results of the examined samples.

| Designatin | Experimental load(KN) | Analytical load(KN) | Nominal load (KN) | $P_{Exp}/P_{ANA}$ | $P_{Exp}/P_{Nom}$ | Hollownes ratio |
|------------|-----------------------|---------------------|-------------------|-------------------|-------------------|-----------------|
| SS1-R00    | 1400                  | 1279.5              | 1276              | 1.09              | 1.10              | 0.704           |
| SS1-R30    | 1250                  | 1271                | 1267              | 0.98              | 0.99              | 0.704           |
| SS1-R60    | 1240                  | 1259                | 1253              | 0.98              | 0.99              | 0.704           |
| SS2-R00    | 1400                  | 1319                | 1301              | 1.06              | 1.08              | 0.528           |
| SS2-R30    | 1395                  | 1306                | 1288              | 1.07              | 1.08              | 0.528           |
| SS2-R60    | 1240                  | 1287                | 1268              | 0.96              | 0.98              | 0.528           |
| SC2-R00    | 1460                  | 1319                | 1301              | 1.11              | 1.12              | 0.528           |
| SC2-R30    | 1400                  | 1306                | 1288              | 1.07              | 1.09              | 0.528           |
| SC2-R60    | 1350                  | 1287                | 1268              | 1.05              | 1.06              | 0.528           |
| SS2-R30-C  | 800                   | 998                 | 988               | 0.80              | 0.81              | 0.472           |

## 8. Conclusion

This research delineates and examines a lab study into the performance and failure mode of sustainable CFDST square columns samples. The experiment's results lead to the following conclusions:

1. Self-compacting concrete mixes exhibit higher compressive strength than conventional concrete mixes. The results show that substitution of recycled concrete aggregate (RCA) improves the filling and passing capacity of SCC by 30% and 50%, respectively, and these mixes exhibit adequate resistance to segregation.
2. The maximum axial strength of CFDST columns is inversely proportional to the void fraction, regardless of the geometry of the column specimens tested.
3. The maximum axial strength of CFDST columns increases with the increase in void fraction for round inner tubes and decreases with the increase in void fraction for square inner tubes.
4. The maximum axial strength of CFDST square columns increases by 4.3% when the square inner tube is replaced by a round tube.
5. The stiffness and maximum axial strength of CFDST column specimens without recycled aggregate concrete are higher than those with recycled aggregate.
6. The bearing capacity of CFDST square columns with concrete aggregate (30% and 60%) decreases by 5% and 10%, respectively.
7. For the same cross-sectional properties (thickness and area), the load-bearing capacity of cold-formed circular CFDST columns is up to 12.5% higher than that of square columns, except for the shape.
8. The maximum axial strength values predicted by experimental and analytical studies for CFDST column specimens were compared. The results of both methods are very close, with the ratio ( $P_{exp}/P_{anal}$ ) averaging about 1.041 for square column specimens and 1.11 for circular column specimens.

## References

- [1] Feng, P., Cheng, S., Bai, Y., & Ye, L. (2015). Mechanical behavior of concrete-filled square steel tube with FRP-confined concrete core subjected to axial compression. *Composite Structures*, 123, 312-324.
- [2] Yu, T., Lin, G., & Zhang, S. S. (2016). Compressive behavior of FRP-confined concrete-encased steel columns. *Composite Structures*, 154, 493-506.
- [3] Xiao, J., Huang, Y., Yang, J., & Zhang, C. (2012). Mechanical properties of confined recycled aggregate concrete under axial compression. *Construction and Building Materials*, 26(1), 591-603.
- [4] Han, L. H., Ren, Q. X., & Li, W. (2011). Tests on stub stainless steel-concrete-carbon steel double-skin tubular (DST) columns. *Journal of Constructional Steel Research*, 67(3), 437-452. <https://doi.org/10.1016/j.jcsr.2010.09.010>.
- [5] Zhao, X. L., & Han, L. H. (2006). Double skin composite construction. *Progress in structural engineering and materials*, 8(3), 93-102. <https://doi.org/10.1002/pse.216>.
- [6] Saleh, S. M., & Majeed, F. H. (2018). Experimental Behavior of High Strength Concrete Filled Double Skin Steel Tubular Columns. *Iraqi Journal of Civil Engineering*, 12(1).
- [7] Aziz, R. J., Al-Hadithy, L. K., & Resen, S. M. (2017). Finite element modelling of concrete filled double skin steel tubular columns under cyclic axial compression load. *Al-Nahrain Journal for Engineering Sciences*, 20(2), 326-340.
- [8] Han, L. H., Tao, Z., Huang, H., & Zhao, X. L. (2004). Concrete-filled double skin (SHS outer and CHS inner) steel tubular beam-columns. *Thin-walled structures*, 42(9), 1329-1355.
- [9] Tao, Z., & Han, L. H. (2006). Behaviour of concrete-filled double skin rectangular steel tubular beam-columns. *Journal of Constructional Steel Research*, 62(7), 631-646.
- [10] Han, T. H., Stallings, J. M., & Kang, Y. J. (2010). Nonlinear concrete model for double-skinned composite tubular columns. *Construction and Building Materials*, 24(12), 2542-2553.
- [11] Dong, C., & Ho, J. (2012, December). Concrete-filled double-skin tubular columns with external steel rings. In *Proceedings of the Australian Earthquake Engineering Society 2012 Conference*, Gold Coast, Australia (pp. 7-9).
- [12] Al-Rekabi, A. H., Al-Marmadi, S. M., Dhaheer, M. S., & Al-Ramahee, M. (2023, July). Experimental investigation on sustainable fiber reinforced self-compacting concrete made with treated recycled aggregate. In *AIP Conference Proceedings* (Vol. 2775, No. 1). AIP Publishing. <https://doi.org/10.1063/5.0140655>
- [13] Al-Rekabi, A.H., and Abo Dhaheer, M.S. (2024). "Performance of Sustainable Fiber Reinforced Concrete with Recycled Aggregates: A Critical Review". *AIP Conference Proceedings*, 3079, 060014-1-060014-10; <https://doi.org/10.1063/5.0202348>
- [14] Al-Rekabi, A.H., and Abo Dhaheer, M.S. (2024). "Flexural performance of sustainable hybrid fibre-reinforced SCC beams made of treated recycled aggregates". *Journal of Building Pathology and Rehabilitation*, 9, 33. <https://doi.org/10.1007/s41024-023-00382-3>
- [15] Wang, B., Yan, L., Fu, Q., & Kasal, B. (2021). A comprehensive review on recycled aggregate and recycled aggregate concrete. *Resources, Conservation and Recycling*, 171, 105565. doi: 10.1016/j.resconrec.2021.105565.
- [16] Yang, Y.-F., & Han, L.-H. (2006). Experimental behaviour of recycled aggregate concrete filled steel tubular columns. *Journal of Constructional Steel Research*, 62(12), 1310-1324.
- [17] Xiao, J., Huang, Y., Yang, J., & Zhang, C. (2012). Mechanical properties of confined recycled aggregate concrete under axial compression. *Construction and Building Materials*, 26(1), 591-603.
- [18] Yang, Y.-F., & Ma, G.-L. (2013). Experimental behaviour of recycled aggregate concrete filled stainless steel tube stub columns and beams. *Thin-Walled Structures*, 66, 62-75.
- [19] Ma, H., Chen, Y., Bai, H., & Zhao, Y. (2019). Eccentric compression performance of composite columns composed of RAC-filled circular steel tube and profile steel. *Engineering Structures*, 201, 109778.
- [20] Yu, F., Chen, L., Bu, S., Huang, W., & Fang, Y. (2020). Experimental and theoretical investigations of recycled self-compacting concrete filled steel tubular columns subjected to axial compression. *Construction and Building Materials*, 248, 118689.

- [21] Liu, Z., Lu, Y., Li, S., & Xiao, L. (2021). Enhanced bond-slip behavior between recycled aggregate concrete and steel tubes under repeated loading. *Structures*, 33, 1263–1282.
- [22] Wu, Z., Ke, X., & Su, Y. (2021). Experimental Performance of Recycled Aggregate Concrete-filled Square Steel Tubular (RACSST) Stub Columns After Exposure to High Temperature and Water Spraying Cooling. *International Journal of Steel Structures*, 21(3), 787–799.
- [23] Iraqi Specification 5. Iraqi Organization of Standards, IQS 5/1984, for portland cement. 1984.
- [24] Bibm, C., & Ermco, E. F. C. A. (2005). EFNARC: The European guidelines for self compacting concrete. Specification, production and use, 63(3).
- [25] Iraqi Specification 5. Iraqi Organization of Standards, IQS 45/1984, for coarse aggregate. 1984.
- [26] Iraqi Specification 5. Iraqi Organization of Standards, IQS 45/1984, for fine aggregate. 1984.
- [27] ASTM A36/36M; Standard Specification for Carbon Structural Steel: Annual Book of ASTM Standards. ASTM: West Conshohocken, PA, USA, 2008.
- [28] ACI Committee 237, “Self-Consolidating Concrete (ACI 237R-07) (Reapproved 2019),” American Concrete Institute, Farmington Hills, MI, 2007, 30 pp.
- [29] HUSSEIN GHANIM HASAN (2020) Compression Performance of Concrete Filled Double Skin Steel Tube Columns”, Ph.D. Thesis, college of engineering, Gaziantep University.